Scanning Microscopy

Volume 1990
Number 4 *Fundamental Electron and Ion Beam Interactions with Solids for Microscopy, Microanalysis, and Microlithography*

Article 14

1990

Electron Stimulated Surface Chemistry

Miles J. Dresser
Washington State University

Scanning Microscopy Supplement 4, 1990 (Pages 193-206) 0892-953X/90$3.00+.00
Scanning Microscopy International, Chicago (AMF O'Hare), IL 60666 USA

Electron Stimulated Surface Chemistry

Miles J. Dresser,

Washington State University, Department of Physics,
Pullman, Washington, U.S.A. 99164-2814
Phone (509) 335-4663

Abstract

When an electron beam of less than 1000 eV interacts with a surface layer a variety of phenomena may occur. In this paper I will discuss those interactions that lead to either chemical changes on the surface and/or desorption of species or fragments from the surface. Theoretical models of electron stimulated desorption, (ESD) will be presented, specifically the Menzel, Gomer, and Redhead model, the Knotek, Feibelman model and the Ramaker, White and Murday model. Experiments that display the angular distribution of the desorbing ionic or metastable fragments, (referred to as ESDIAD for Electron Stimulated Desorption: Ion Angular Distributions) are the primary emphasis. The process of electron beam induced conversion of CO on metal surfaces (Pt (111) and Ni (110)) with the emission of O^+, CO^+, and CO* from the surface as seen in ESDIAD experiments shows a change of phase of the surface CO on the nickel surface above 0.75 CO/Ni and an interesting change in the bonding configuration in the coverage range of 0.50 - 0.66 CO/Pt on the platinum surface.

The ESDIAD data show that NH_2 adsorbed on the silicon (100) reconstructed surface yields a very broad elliptical ESDIAD distribution that is peaked normal to the (100) surface and oriented with its major axis perpendicular to the Si surface dimers. The hydroxyl group, OH, has a four beam ESDIAD pattern that indicates off normal orientations for the H bond of OH on Si (100). Fluorine is emitted from the Si (100) surface along the direction of the Si dangling bond.

The conversion of NH_3 to NH_2 on Ni (110) is a beam induced effect in a surface layer as seen by ESDIAD. The electron beam dissociates the NH_3 by releasing an H^+ ion and leaving NH_2 which produces a two lobed ESDIAD pattern. The conversion of PF_3 (another surface rotor) to PF_2 and PF on Ni (111) surfaces is manifest in a six lobed ESDIAD pattern that rotates 30° and acquires a strong central beam as a result of electron bombardment. These ESDIAD beams are correlated with bonding orientation and sites for PF_2 and PF on the Ni (111) surface.

The surface spectroscopy of electron energy loss spectroscopy, EELS, is presented to demonstrate the electron beam induced decomposition of dimethyl and difluoromethyl ether on an alumina (Al_2O_3) surface. The resultant surface species from the fluorinated ether appears to contain a very stable form of an Al-F bond.

Key Words: Electron Stimulated Desorption, Ion Angular Distributions, Electron beam induced effects, Chemisorbed layer, Cross sections, Surface intermediates, Excited Surface Species, N_2, NH_3, CO, PF_3, F_2, Hydrocarbons, Alkyl Ethers, Ni, Ru, Si, Al, AL_2O_3.

Introduction

The study of surface changes as a result of electron bombardment has been pursued actively for about 30 years. About ten years ago several experiments were accomplished that were extremely fruitful in terms of developing a fundamental understanding of the phenomena. In this paper I would like to review first the current interpretation of processes that we feel are understood in the low energy (<1000 eV) regime and their significance. This field is fraught with acronyms and I will try to define them carefully as we proceed. We are going to study the general area of Desorption Induced by Electronic Transitions, DIET, but more specifically the subfield of Electron Stimulated Desorption, ESD. Our focus is broader than these later two categories because we will look not only at desorption processes but surface excitations that may lead to chemical changes on the surface. After discussing the fundamental models of ESD I will describe experiments that display important new surface interaction phenomena as seen by the analysis of the angular distribution of the desorbing ionic fragments, ESDIAD, (for Electron Stimulated Desorption: Ion Angular Distributions). The process of electron beam stimulation of CO on metal surfaces (Pt and Ni) leading to the emission of O^+, CO^+, and CO* demonstrates the fundamental excitation of a covalent bonded species and this becomes a powerful tool for observing different surface phases of CO through the angular orientation of the surface molecules. The usefulness of the ESDIAD technique for determining molecular orientations on the silicon (100) reconstructed surface will be displayed with the specific examples of NH_2, OH and F. These surface species are all the result of a hydrogen detachment from the molecules NH_3, H_2O, and HF. The conversion of NH_3 to NH_2 on Ni (110) becomes an example of a more profound beam induced change of a surface layer (this process is seen on other metals as well). The conversion of PF_3 (the surface rotor) to PF_2 and PF on Ni surfaces is a similar example. The surface spectroscopy of electron energy loss spectroscopy, EELS, will be discussed to demonstrate corroboration of the interpretations given above and to demonstrate some electron beam induced effects on insulating surfaces such as alumina (Al_2O_3).

Theoretical Models of ESD

The simple observation of this phenomenon is that if we direct electrons in the energy range of 10 - 1000 eV onto a surface covered with some sort of molecular species, molecules or molecular fragments are seen to be ejected from the surface, see Fig. 1. These fragments may be ionic or neutral and are sometimes in excited states as well as the ground state.

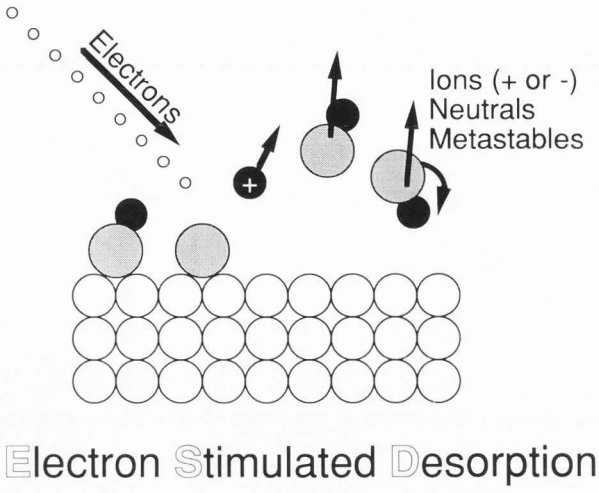

Fig. 1 The observed effect of ESD of an adsorbed layer. The incident electrons produce particles that leave the surface, they may be either ionic or neutral and they may be in ground or excited states.

The first temptation in this field is to think of the electron impact as a mechanical collision in which the momentum and energy of the incident particle are transferred to the adsorbed molecule and it, (or a fragment of it), is thereby blasted from the surface. A few simple calculations for this sort of collision process quickly reveals that the mass difference between the electron and any adsorbed atoms is so large that incident energies in excess of 10 keV are required to provide the energy necessary to fragment or remove the adsorbed species. Since the ESD process proceeds easily at 100 eV there is necessarily a different explanation.

The recognition that electron stimulated desorption may be viewed as an example of a Franck-Condon transition to a dissociative state that is also a desorptive state from the surface was first presented by two separate laboratories, Paul Redhead of NRC (Canada)[22] and Dietrich Menzel and Bob Gomer of the Univ. of Chicago[18]. That description has subsequently become known as the "MGR" model. In this model the incident electron collides with the electrons of the adsorbed species (usually a valence electron) so that our emphasis is now turned to electron - electron collisions. The time scales are important to note here. If the excited electron is in a valence band its life time will be extremely short, on the order of fs (10^{-15} s), because of the band width (typically several eV). This is extremely fast relative to the time scale of nuclear motion so that we can expect that no significant changes in position, momentum, or kinetic energy of the molecules can occur during the time of an electronic transition. These are the assumptions of the Franck-Condon model for molecular excitation and they are seen most easily, (see Fig. 2), on an energy level diagram as vertical transitions to states of common momentum (or kinetic energy). In the drawing a ground state potential curve is drawn with a possible wave function superimposed on the lowest energy level. The vertical transitions predominantly lie between the dashed vertical lines, and the particle then gains kinetic energy as it departs the surface along the reaction coordinate. The distribution in kinetic energy of the departing particle is then a reflection of the initial states spatial distribution of that particle.

The electronic excitation that produces this change is now thought to be either a 1h1e (1 hole, 1 electron) valence transition to a neutral state or a 1h valence transition to an ionic

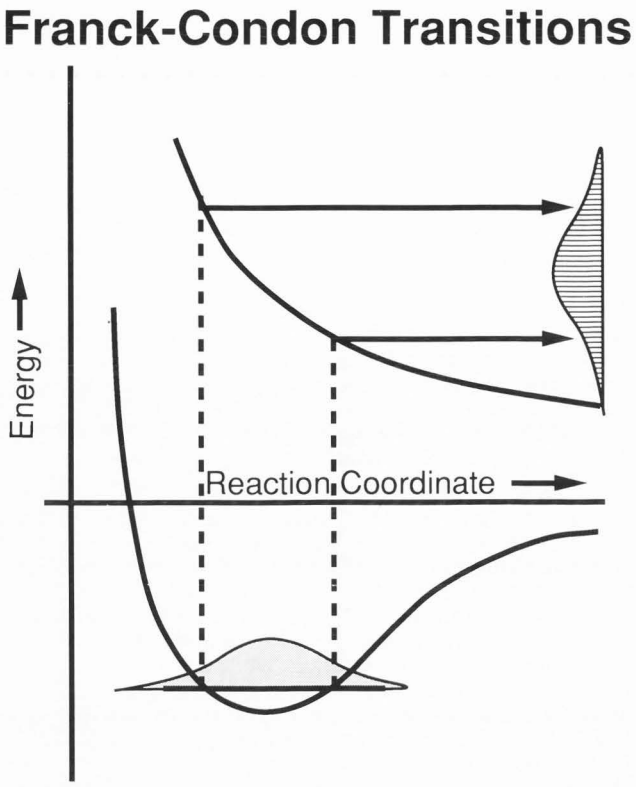

Fig. 2 A sketch of the energy diagram for a molecule bound to the surface, showing one of many possible excited electronic states (this one is antibonding) and the Franck - Condon region for transitions.

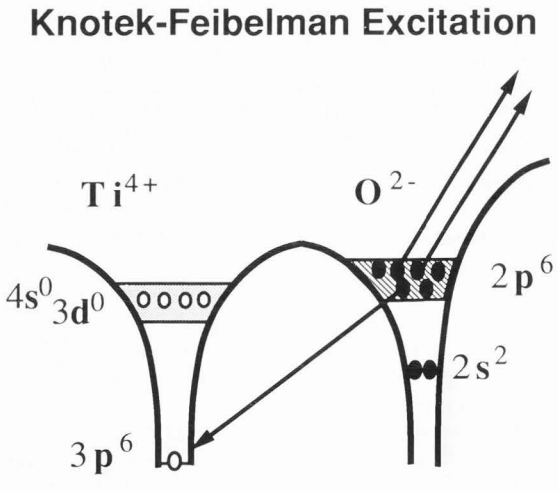

Fig. 3 A sketch (not to scale) of the energy levels involved in an inter-atomic Auger transition that neutralizes the Ti corehole and leaves the oxygen moiety in a positive charge state.

Ultrahigh Vacuum Apparatus for Silicon Surface Chemistry

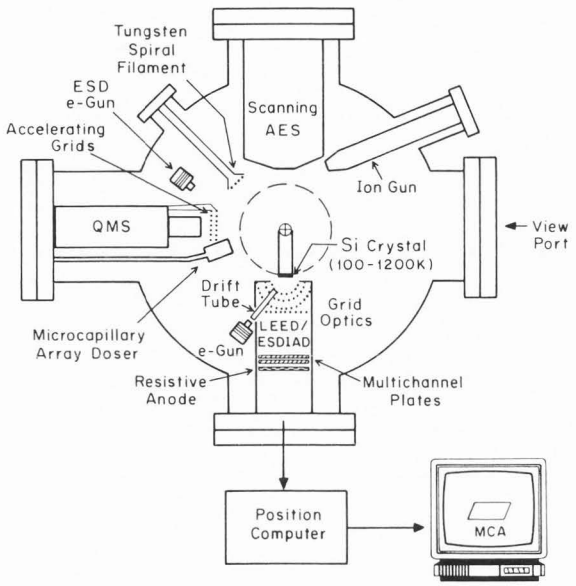

Fig. 4 A typical ESDIAD experimental system[13]. A variety of experimental measurements are available to help determine the nature of surface processes.

state of the adsorbed species. In the initial presentations of the MGR model, the emphasis was on the desorption steps so that the focus on details of the excitation were minimal. Currently there are two other categories of excitations that have been proposed that are usually laid out in contrast to this simple excitation, first the Knotek-Feibelmann[14] inter-atomic Auger transition with the release of multiple electrons to create an antibonding ionic moiety, and secondly the 2h or 2h1e excitations on covalently bonded materials as discussed by Ramaker, White, and Murday [21]. All of these excitations may be to repulsive states and thus become the mechanism leading to desorption, but they may also lead to states that dissociate on the surface thus changing the chemical character of the surface species.

In 1978 Knotek & Feibelmann proposed their model of excitation for the ESD of O^+ from TiO_2 [14]. Since the oxygen is bound to the titanium as a 2^- ion there was an initial puzzle as to the mechanism for losing the three electrons to go from O^{2-} to O^+. The explanation of this was that the incident electron created a corehole in the titanium atom (as measured by the threshold). As a result of this an interatomic Auger decay followed, (see Fig. 3), that involved the dropping of one electron from the oxygen into the Ti corehole and the simultaneous ejection of two or more electrons from the oxygen valence levels to the vacuum. For this system the resultant excitation is then a 1h positive ion state for the oxygen sitting in what was a negative ion site. The reversed Madelung potential then drives the charged oxygen moiety from the surface in a process that has been called a "Coulomb Explosion" (for molecular dissociation) and is recognized as the ion's moving out along the repulsive potential portion of our Franck-Condon picture.

Cross-sectional View of
Digital LEED/ESDIAD Apparatus

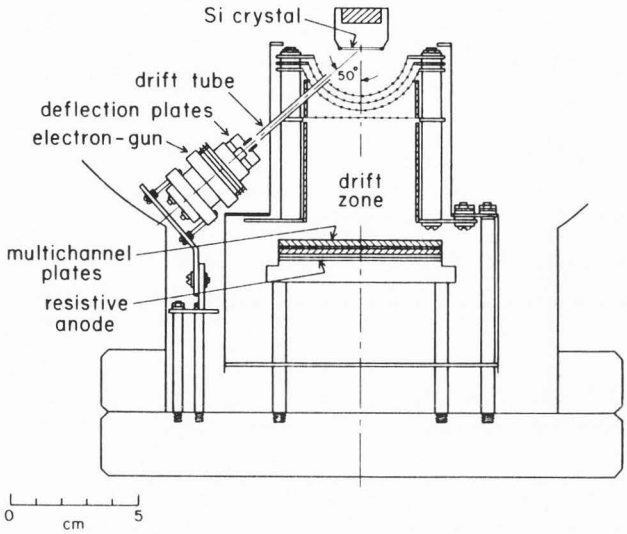

Fig. 5 The detail of a typical ESDIAD/LEED analyzer[13]. The electrons are directed from the electron gun onto the crystal surface. The resultant desorption products move out toward the hemispherical grids and on to the multi-channel plates, (MCP), where they are amplified and input to a position sensitive detector that can determine the incident (x,y) coordinates of that particle on the MCP. These events and their coordinates are accumulated in computer memory for approximately 10^5 events in a 128 x 128 array.

More recent work has shown the importance of another mechanism in covalently bonded surface species. Ramaker, White, and Murday have shown the importance of 2h and 2h1e excitations in ESD processes[21]. The important fact related to these excited states is that these electronic excitations are to localized wavefunctions which correspond to longer lifetimes. The lifetime is sufficiently long that the excited surface moiety can be repelled by that 2h or 2h1e state long enough to initiate separation from the surface.

The previous discussion has focused on the excitation mechanism for the process, however, the details of the subsequent desorption are also of importance. The desorbing particle is usually ejected along a path that is along the direction of the bond (the reaction coordinate) that had held the molecule or molecular moiety prior to the excitation step. This observation has been experimentally confirmed in a wide variety of cases including collaboration with low energy electron diffraction (LEED), and angle resolved ultraviolet photoelectron spectroscopy (ARUPS). The process has also been theoretically modeled and shown to yield distributions that are peaked in the direction of the peaks of the initial state wave functions. There are, however, two important modifications that must be recognized that cause distortions in the apparent bond directions of departing particles. The first of these is the *image potential*. The image potential is present for all departing charged particles. The effect will be strongest for particles leaving from conducting surfaces. Since a charged particle outside a conducting plane induces a redistribution of charge in the plane that is most simply described by the construct of an oppositely charged entity equidistant beneath the surface called the image, both the original charge and its image will attract each other. This

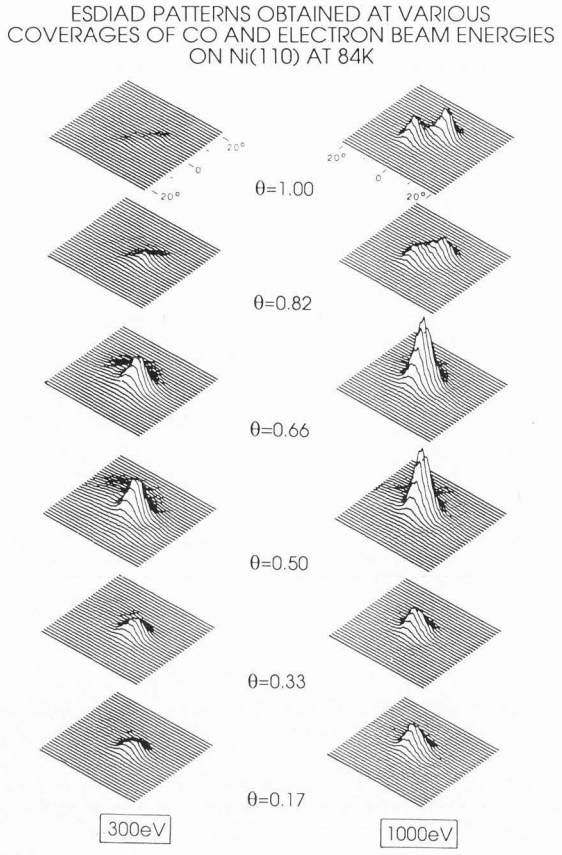

Fig. 6 ESDIAD data for CO on Ni(110)[1,11]. The distributions shown are the O^+ yields for progressively larger coverages of CO. The incident electrons have an energy of 300 eV or 1000 eV, and the surface is at 84 K.

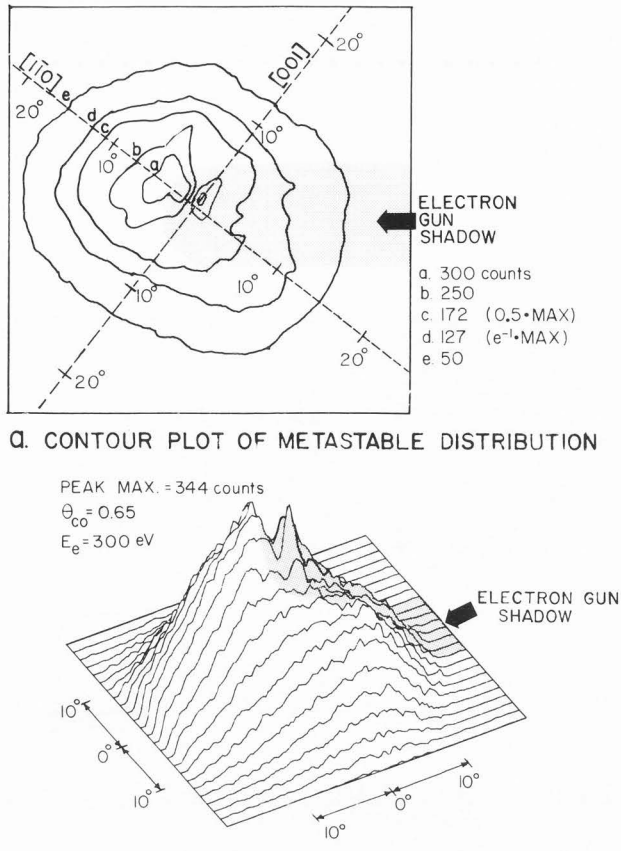

Fig. 7 The angular distribution of the $a^3\pi$ CO (metastable) from Ni(110)[2]. These data were taken with the incident electron energy of 300 eV and the surface at 84 K.

attractive force will deflect the particle quite significantly in its initial trajectory thus making the peaked distribution occur at larger angles when they are detected than the angle from which they were released. The second effect is *reneutralization* which occurs for departing charged particles as they experience potential energy curve crossings with neutral state potential energy curves. As the particle desorbs from the surface there is a finite probability that the desorbing charged species can be reneutralized by the adsorption or release of an electron. The probability of reneutralization falls off exponentially as the particle separates from the surface. The reneutralization of ESD ions is a large effect, only about 1 out of 10^2 to 10^3 excited particles will escape as ions. Thus wide angle releases will more likely be reneutralized than more normal emissions. This causes the peak of the distribution to appear to lie at smaller angles from the surface normal. The magnitude of the distortions caused by these two effects has been calculated by Miscovick et al.[19] and they discovered that the two effects are close to self canceling out to about 30°. Both of these effects will produce errors in the estimate of polar angle but the azimuthal distributions of departing species are not likely to have distortions from these effects. Thus the angular distribution of released particles can give important information regarding the initial molecular orientations on the surface.

Electron Stimulated Desorption Studies

The first group of experiments that I would like to show is the ESDIAD of CO on Ni and Pt surfaces. Carbon monoxide on the Ni (110) surface yields several interesting results[1,11]. First note briefly the experimental apparatus in Fig. 4. This is performed in an ultra-high vacuum chamber that typically has base pressures of 2 nPa ($3x10^{-11}$ Torr). Calibrated beam dosers are employed to ensure that surface coverage of introduced species can be known on an absolute basis to better than 10% (some of the older experiments are known to about 20%). The chambers also provide mass spectrometers so that particular gases can be monitored and a variety of tools for ensuring that the surface is clean and properly characterized such as AUGER analyzers, ion sputtering, and temperature control for heating to incandescent temperatures or cooling to liquid nitrogen temperatures. A sketch of the ESDIAD/LEED analyzer is shown in Fig 5. Here electrons from the electron gun strike the surface and activate surface adsorbed species. Particles that are ejected from the surface then travel toward the detector. Positive ions are further accelerated by an attractive voltage on the hemispherical grids. The planar grid then accelerates the positive ions even more strongly so that their angular distribution is projected back to the input side of a pair of multi-channel plate, (MCP), amplifiers. The output side of the

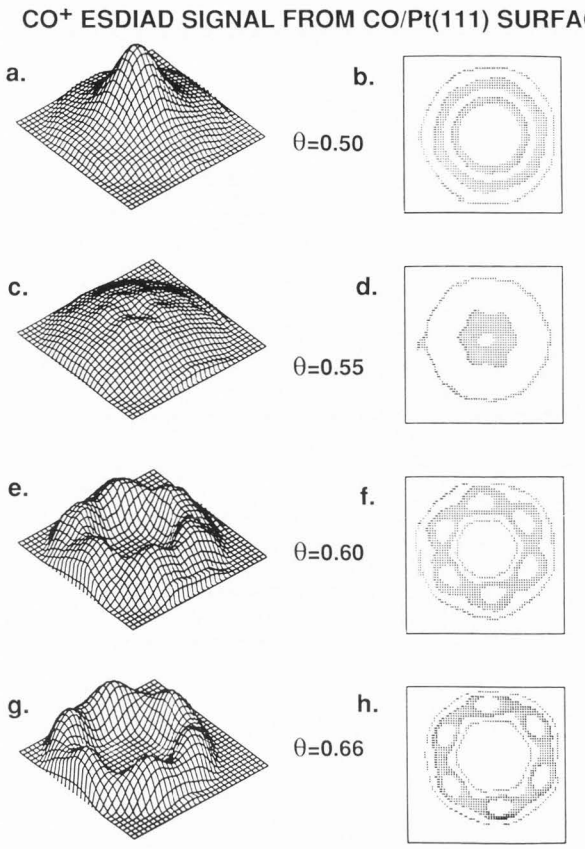

Fig. 8 ESDIAD data for CO on Pt(111)[17]. The distributions shown are the CO^+ yields for progressively larger coverages of CO. The incident electrons have an energy of 260 eV, the surface is at 90 K, and there is no crystal bias

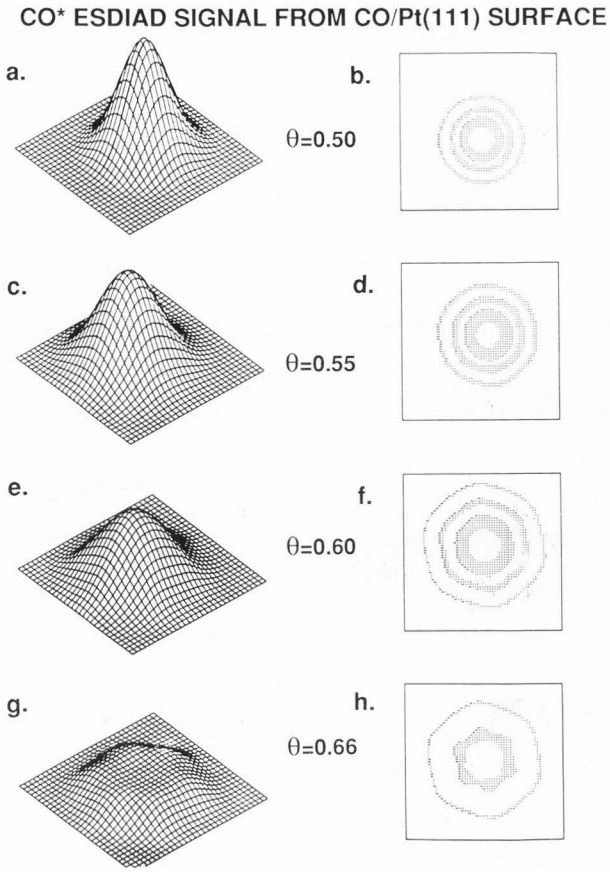

Fig. 9 ESDIAD data for CO on Pt(111)[17]. The distributions shown are the CO^* yields for progressively larger coverages of CO. The incident electrons have an energy of 260 eV, the surface is at 90 K, and there is no crystal bias

MCP ejects an electron burst which is collected on a thin conducting square film. The pulse height at the corners of the film can be used to calculate the x-y coordinates of the incident ion on the input plane of the MCP. This data pair is stored as a single event and accumulated for about 100,000 counts in computer memory for subsequent display and analysis. This data accumulation takes about 3 minutes with incident electron currents in the order of 1-10 nA. LEED data can also be taken for this surface by reversing the polarity of bias on the hemispherical grids. The nature of the CO surface layer on Ni (110) surface is known from both LEED and ESDIAD measurements. The Ni (110) ideal surface consists of rows of atoms in the $(1\bar{1}0)$ surface direction. These rows are separated by parallel valleys. CO is known to adsorb on top of these rows with a preference for the top of the individual surface atoms. As the surface coverage is increased the density of molecules along these rows becomes more closely packed up to a point of 0.75 CO/Ni where a dramatic change is noted. Figure 6 shows the ESDIAD pattern for O^+ ions (dominantly) from a CO layer as a function of coverage. Note that above a coverage of about 0.75 CO/Ni the ESDIAD pattern shows the development of a double beam pattern. This signifies the formation of regions where the CO is tilted as opposed to normal on the surface. Note that the tilting is immediately seen at the angle of approximately 19° it does not progressively tip over. This suggests that the tilted molecules are forming in islands such that there are regions of the tilted phase and regions of the upright phase. As coverage increases the islands of tilted species grow at the expense of the regions of upright species. Thus we see a phase transformation that occurs at 0.75 CO/Ni. Our attention was focused on the O^+ emission in the previous experiment but we should note that under electron bombardment three species (O^+, CO^+, CO^*) of released particles can be seen in this apparatus and a fourth species (the CO neutral) can be seen with other techniques. The angular distribution of CO^*, (see Fig. 7), is about the same as that of O^+, (fwhm in the (001) direction is 15°), but the angular distribution of CO neutrals is much broader (fwhm~30°)[2]. There is an asymmetry in the metastable distribution that is seen as an elongation of the pattern in the direction along the Ni (110) surface rows (in the $(1\bar{1}0)$ direction fwhm is ~22°). This asymmetry is interpreted as an enhanced ability for reneutralization for particles traveling parallel to the rows. There is a corresponding elongation in the ionic distributions in the direction transverse to the rows. Thus the picture from the nickel data is that the CO^* and CO^+ arise from a common excitation to a 2h1e state such as the $5\sigma^{-1}1\pi^{-1}2\pi_a$, as this excited moiety begins to separate from the surface it may be reneutralized to $5\sigma^{-1}2\pi_a$ which becomes the $a^3\pi$- CO metastable state.

The ESDIAD studies of CO on platinum (111)[16,17] also provides some interesting results for the understanding of

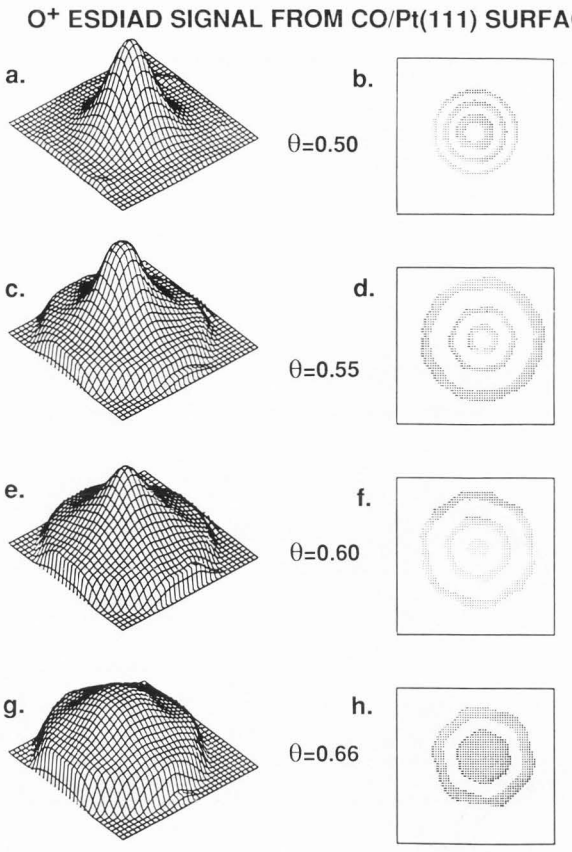

Fig. 10 ESDIAD data for CO on Pt(111)[17]. The distributions shown are the O^+ yields for progressively larger coverages of CO. The incident electrons have an energy of 260 eV, the surface is at 90 K, and there is no crystal bias

surface layers on metallic substrates. The three species CO^+, CO^*, and O^+ can be separated by the use of retarding potentials in the ESDIAD analyzer[16]. The mean energy for CO^+ ions is ~1eV and for O^+ ions it is ~4eV, thus a retarding potential of 1.5eV will only pass O^+ ions or metastables and a retarding potential of 7eV will only pass metastable species. If one takes differences of the ESDIAD patterns thus acquired, resultant patterns due to the three species are thereby possible. In Fig. 8 the pattern for CO^+,[17]is shown in the coverage range of 0.5 CO/Pt to 0.66 CO/Pt. The left hand frames (a, c, e, g) show the three dimensional projection plots and the right hand frames (b, d, f, h) show a contour plot of the corresponding distribution. These data were taken with no potential between the crystal and the first grid to maximize angular detail for these strongly focused beams. Below 0.5 CO/Pt the pattern is of similar shape to that of frames a and b but of decreasing amplitude. The coverage of 0.66 CO/Pt is one monolayer for this system. The pattern evolves from a central normal beam to six beams that are directed away from the normal by 14°. The six beams are in the six surface directions equivalent to $[1\bar{1}0]$.

The comparable data for CO^* are shown in Fig. 9 where a somewhat similar result is seen although the six off axis beams are not as strong as they were for CO^+. These beams only lie 6° off of the normal.

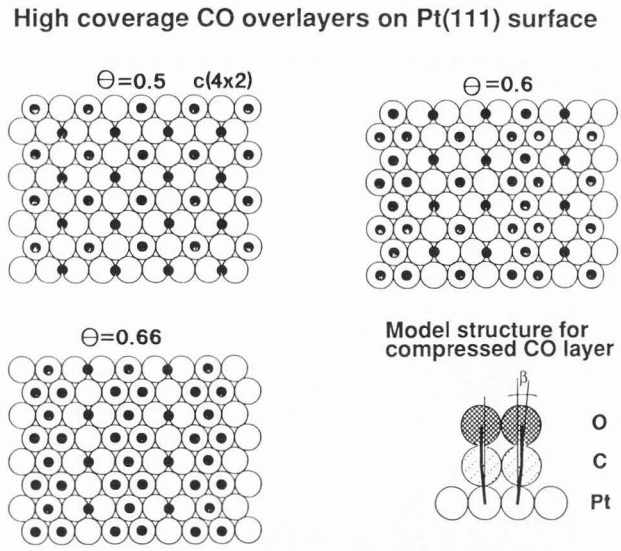

Fig. 11 (a-c) The structural model for compressed CO layers on Pt(111) proposed by Avery[6]. (d) Schematics of the tilted terminal-CO molecules building the edges of the fault lines.

The remaining species O^+ is displayed in Fig. 10 where the pattern shows a broadening of the central peak and a weak hexagonal symmetry evident in the contour plot. Our model of this behavior can be seen in Fig. 11 where the surface coverage patterns proposed by Avery[6] from LEED data are shown for the coverages of these data. Frame d of Fig. 11 shows the compressed packing of CO thus inducing the 6° tilt observed in the CO^* data. It is presumed that the 14° tilt observed in the CO^+ data has been expanded by image force effects. Because of the hexagonal substrate symmetry there will be three possible different domains of this arrangement thus leading to the six beam patterns observed. Again we have seen that the result of close packing of CO on a metal surface leads to a configuration of tilted molecules. This is another surface phase change. In the platinum work the CO^+ and CO^* can be shown to come from different excitations rather than the single excitation postulated in the nickel data. Kiskinova et. al.[16] have shown that CO^+ is released only after excitation of a bridge bonded species while CO^* and O^+ are seen to come from either bridge or terminally bonded CO. Thus the CO^+ pattern displays the tilting phenomenon most clearly.

I will next look at the ESDIAD results from a silicon surface. To date only a few species have been studied by ESDIAD on the silicon surface. These molecules include the first-row protic hydrides, that is NH_3, H_2O, HF[13,15] as well as fluorine[8]. All of these species adsorb on silicon dissociatively by the detachment of one of their hydrogen moieties. The remaining fragments, (i.e. NH_2, OH, and F) attach to the dangling bonds on the free ends of the reconstructed silicon surface dimer. Figure 12 shows a ball model construction of (A) the Si(100) surface (unreconstructed) and (B) is the surface after reconstruction. Since the silicon atom is normally bonded in a tetragonal configuration, it can be seen that one of the two upper bonds tilts to the neighboring silicon and shares one of its bonds in reconstruction. Thus there is one free dangling bond for each Si surface atom. The HF work and the fluorine work both image this dangling bond. Figure 13 shows the digitally acquired data of Johnson et al.[15] (Panel (a)) and the phosphor

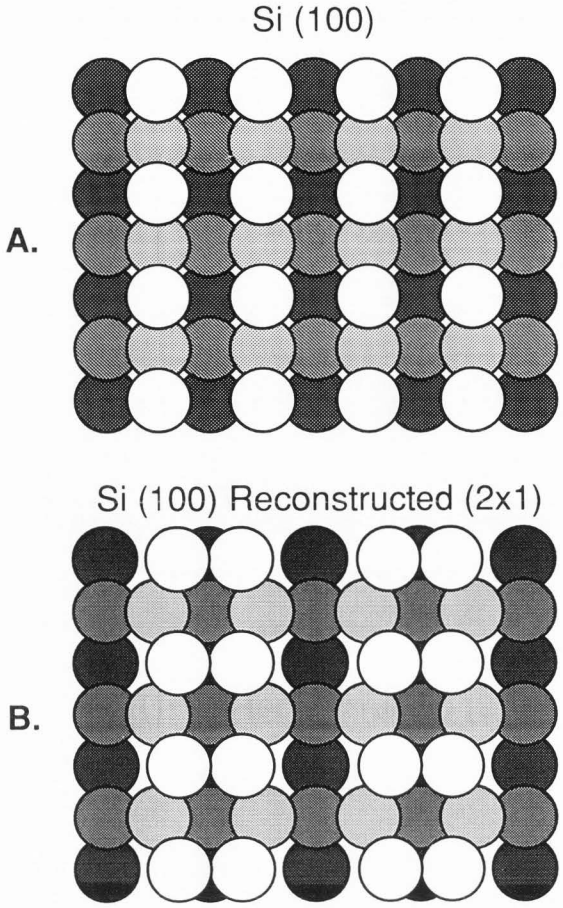

Fig. 12 A ball model view looking down on the top of the (100) silicon surface. Frame A shows the surface as it would be if it had the same configuration as the bulk. Frame B shows the reconstructed surface in which adjacent rows of surface atoms are drawn together to form dimers. Progressively darker shades of gray correspond to deeper layers of silicon.

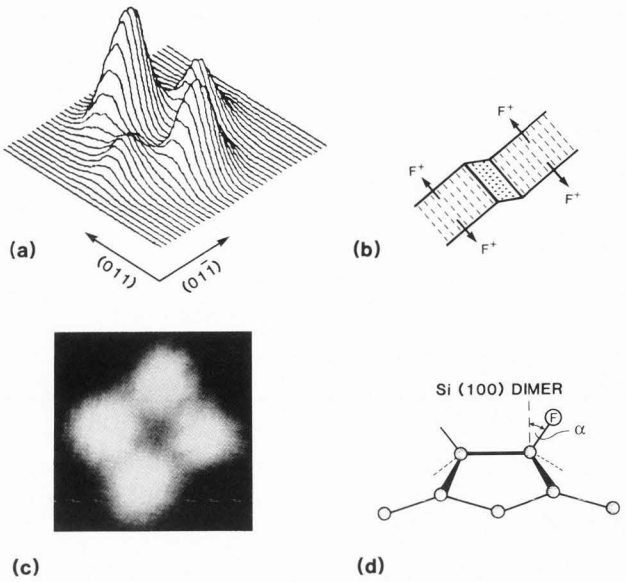

Fig. 13 ESDIAD data from fluorine on Si. Panel (a) shows the HF data of Johnson et al.[15] and the Panel (c) shows the impurity fluorine data of Bozack et al.[8] in the phosphor screen method of data presentation. Panel (b) shows the dimer orientation on a stepped surface, and Panel (d) shows the proposed bonding angles with silicon dimers.

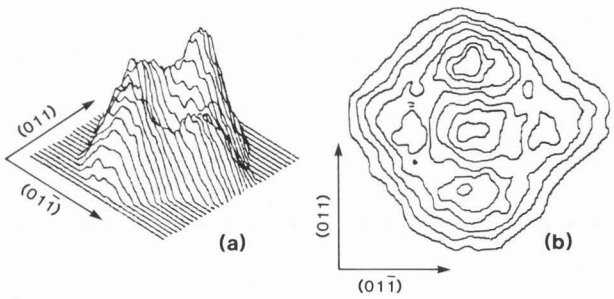

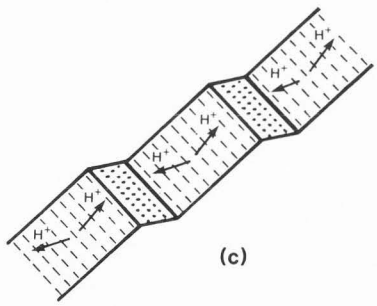

Fig. 14 The angular distribution of released H^+ from OH on Si(100). Data from Johnson et al.[15].

screen data of Bozack et al.[8] (Panel (c)). The weighted average of both the Johnson et al. and the Bozack et al. measurements gives an angle of 32°± 3° from the surface normal for the fluorine bond direction. This is thought to be a measure of the dangling bond direction. While the intensity of the spots in the Bozack et al. data look fairly equal the preference of the intensity along one axis versus the other axis of the Johnson et al. data shows that their surface is different. The Johnson et al. surface was a vicinal Si(100) surface, that is, it was cut a few degrees off of the exact (100) direction. Surfaces cut in this manner are found to form plateaus of (100) with the dimers all parallel to the step ledges (see Fig. 13 Panel (b)). Thus a preponderance of a particular dimer direction is found in this surface, and we see that the Fluorine peaks in the ESDIAD data shows that preference. This observation also suggests that the Bozack et al. data corresponds to a surface with domains of either orientation in relatively equal populations. Johnson and co-workers also measure the fwhm of these beams at 130K to be 19° [15]. This is slightly wider than the CO beams from metals in our earlier discussion but is roughly the same size. Also note that only a very small amount of H^+ ions are seen in experiments where the ESD signal from HF is directed into a quadrupole mass analyzer. Thus the electron stimulation of Si-H bonds does not lead to H^+ emission.

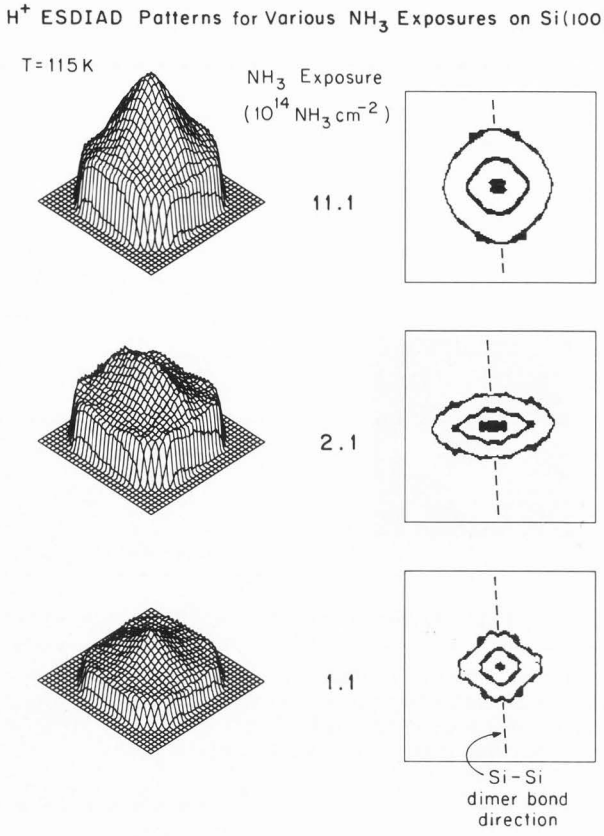

Fig. 15 The angular distribution of H^+ released from NH_3 on Si(100)[13]. The incident energy is 300 eV and the surface temperature is 115 K.

The ESDIAD patterns for OH appear quite similar to those of HF[8], (see Fig. 14), However the pattern is rotated 90° compared to the previous patterns indicating that the dominant ion release is more at right angles to the dimer axis as opposed to parallel to it as was seen in the F^+ data. Analysis of the ion release by mass spectrometry shows that the release here is predominantly H^+ ions. It is inferred that these ions originate from OH species because if one saturates the surface with atomic hydrogen only a marginal H^+ signal can be measured and no hydrogen signal was seen from HF. Thus we find that the Si-H bond is not very ESD active. In data where we see prolific H^+ ion signals the origin of the H^+ signal is most likely from species other than Si-H, in this case from the OH group. Because the beams are at right angles to the dimer direction Johnson et al. propose a dative bond between one of the oxygen lone pairs and a nearby silicon dangling bond, thus pinning the OH moiety so that the H is nearly at a right angle to the dimer direction[15].

The ESDIAD of NH_3 from Si(100) has been reported by the University of Pittsburgh, Surface Science Center[13] as well as the results given in Johnson et al.[15]. The "Pitt" studies identify the surface species as being NH_2 and H from NH_3. Their work also demonstrates more complete data on the coverage for which certain patterns can be found. Figure 15 shows the nature of the ESDIAD data as a function of coverage for the University of Pittsburgh results. Here the most striking feature is that the beam is not in a sharply defined direction but rather in a very wide angle distribution

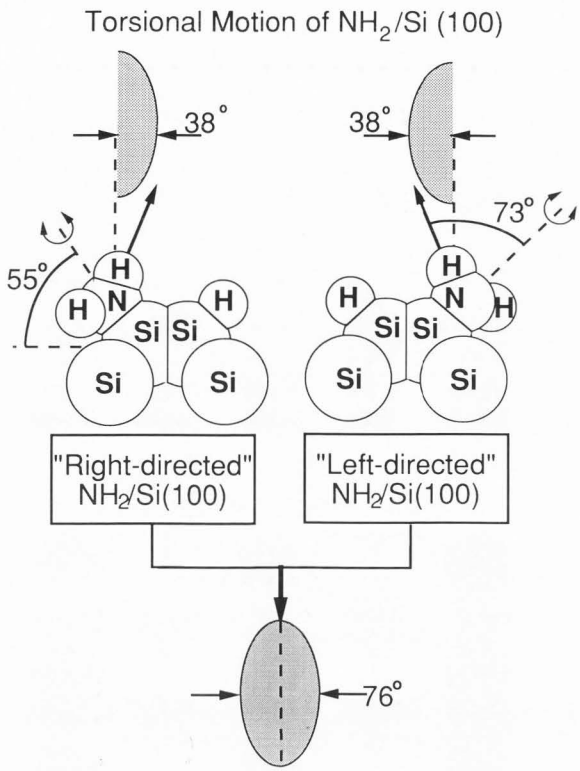

Fig. 16 A model for the release of $H^+$from the NH_2 surface moiety.

and with an elliptical cross section. The data here have been taken at a much weaker crystal bias, (+10V), than the previous data to give us more local detail in the peak. Thus, we also have a larger significant signal at the edges of the detector. This surface has been sufficiently annealed that LEED studies shows that it has a strongly preferred orientation in a single direction. Although the crystal was cut as close to (100) as was possible, (the uncertainty in orientation is ±1°), this surface, like the vicinal surfaces, shows a fixed orientation that does not change with heating or sputtering. While this surface may be the result of slight misorientations in the cut it at least provides broader plateaus between the steps and seemingly smaller domains of misoriented regions. It certainly makes a repeatable and easily characterized surface for study. The Pittsburgh model for these data suggests an NH_2 orientation as shown in Fig. 16. With this model one proposes that the NH_2 is free to rotate around the N-Si bond direction and that the hydrogens that are bound to the nitrogen can then spray out in a broad ridge transverse to the dimer direction and ~38° off of the surface normal . This model helps to make the extremely broad patterns as well as the ellipticity for H^+ more understandable. Other first row protic hydrides have not been studied although it is known that

Fig. 17 The ESDIAD data for NH_3 on the Ni(110) surface[12]. The surface temperature is 85 K and the electron energy is 300eV. Frames a and e show the phosphor screen display. Frames b and f show the raw digital data. Frames c and g show the pattern before and after a long exposure to the electron beam. Frames d and h show ball models of the configurations postulated to explain the data observed.

17A.

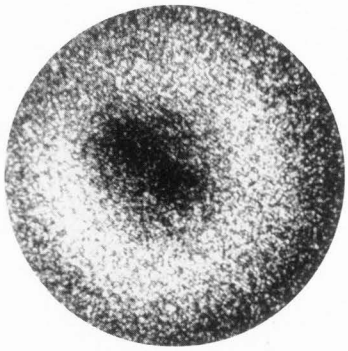

E.

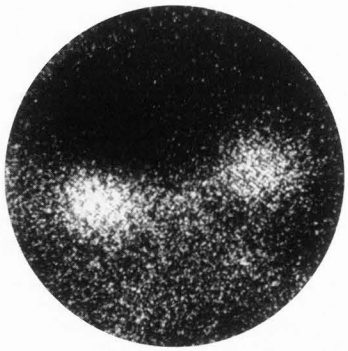

B.

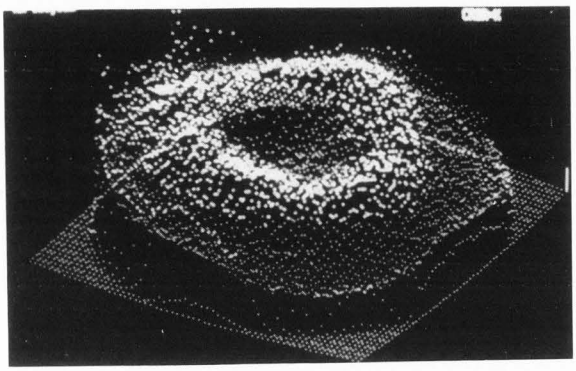

F.

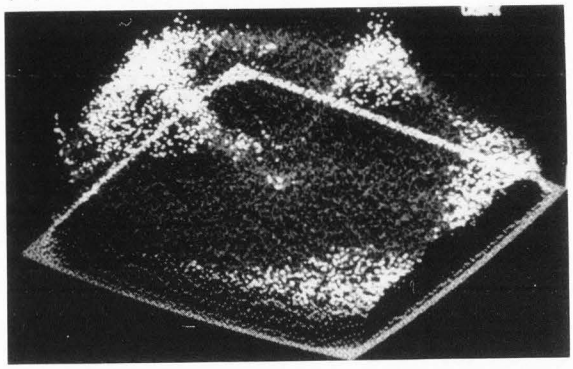

C.

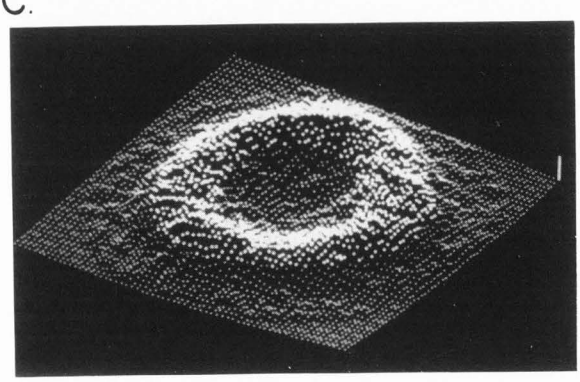

G.

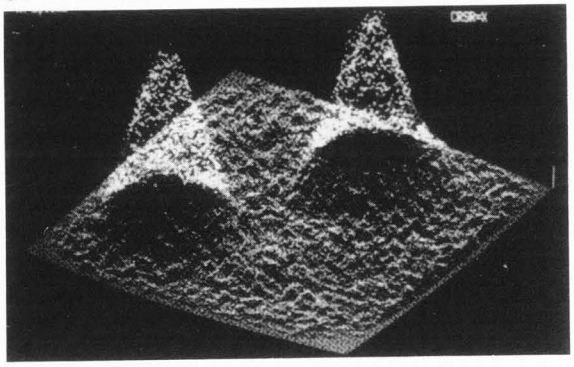

D.

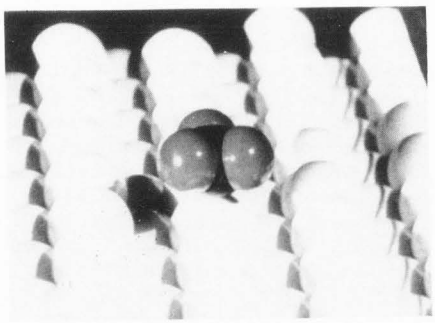

H.

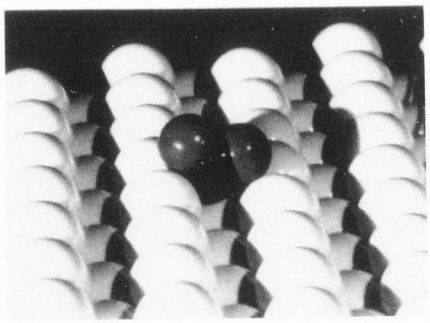

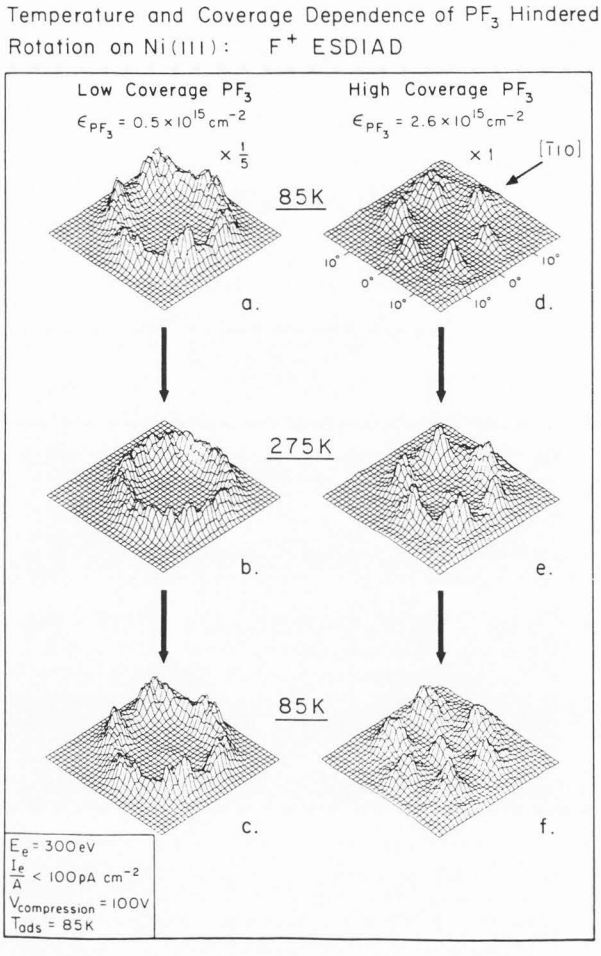

Fig. 18 ESDIAD results for PF_3 on Ni(111)[3] is shown in Frames a-d for different heat treatments and coverages.

methane will not adsorb on Si(100)[9]. While all of these studies are in effect electron beam induced chemistry because the released particle that is imaged is also evidence of a changed chemical composition of the surface layer, there are some beam induced effects that are a more profound sign of surface changes under electron beams. The next section will address those issues.

Electron Beam Effects

In this section we will begin by looking at the decomposition of NH_3 on the Ni(100) surface. Figure 17A shows an acquired set of data for the case of ammonia adsorption on a metal surface[12], (Ni(110)). Note the ring pattern that is evident in frames A, B, and C of these data. Frame A represents the data acquired on a phosphor screen. Frame B represents the raw data as it was collected in the digital apparatus. Frame C is a processed set of data where background effects have been subtracted out and a smoothing procedure has been applied. This ring pattern has been observed and reported several times[4] and is commonly referred to as the "ammonia halo". The model that explains this result is one in which the NH_3 sits atop the ridge of the nickel surface with the nitrogen bonding through its lone pair to the Ni surface. In this orientation the three hydrogens lie above the nitrogen with bond angles that lie 70° from the surface normal. Thus the ammonia C_{3v} axis is parallel to the surface normal. The azimuthal orientation is evidently not in registry with the surface, so that either the NH_3 is spinning or its azimuthal orientation is random. If one continues to watch this pattern as a function of time of exposure to the electron beam, one finds that the pattern makes a dramatic change from the "halo" to a two beam pattern seen in Fig. 17 E-G. Except for the additonal electron bombardment these data are taken in the same manner as that in Frames A-C Alvey et al[4] have explained this change as a result of the loss of one hydrogen moiety with ESD leaving an NH_2 remaining on the surface. Ball models that are consistant with these data are show in Fig. 17 Frames D and H. The observation of electron beam conversion of NH_3 to NH_x was first reported by Danielson et al.[10]. Continuous bombardment leads to the ultimate conversion of most NH_3 to NH_2 on the surface thus the pattern with two beams is characteristic of NH_2 on the surface. Alvey et al[4] have done extensive coverage measurements to ascertain that the appearance of a strong double beam pattern occurs when the surface fragment was, in fact, dominantly NH_2 rather than NH. Further bombardment can lead to a surface where NH is dominant. Electron Energy Loss Spectroscopy, (EELS or HREELS for high resolution EELS), is an important adjunct to these experiments. In this technique fairly low energy electrons are directed in a beam onto a surface. As these electrons scatter from the surface, those that experience inelastic energy loss with the surface have a structure in their energy distribution that typifies the allowed excitation energies of the surface, (including any adsorbed species). Bassignana et al.[7] have studied the NH_3 on Ni(110) system with HREELS and observed frequencies of energy loss that are correlated with NH_2 characteristic frequencies at first, followed by progressively more NH, or ultimately to only N-Ni and H-Ni vibrational frequencies.

A similar but most interesting case is that of PF_3 on the Ni(111) surface. Alvey and Yates[3] have shown that this molecule binds to the surface via the phosphor atom again with its C_{3v} axis normal to the surface. Thus the fluorine atoms lie bonded at angles that are at roughly 70° from the surface normal. At liquid nitrogen temperatures (85 K) the molecule gives a pattern that is shown in Fig. 18 frames a and d. Low coverage data is displayed in frame a of Fig. 18 and high coverage in frame d. Note that the data has a more localized beam character than the NH_3 "halo" particularly in the high coverage case. The sixfold symmetry is correlated to the six fold symmetry of the substrate. When the surface is heated to 275 K the low coverage pattern becomes a "halo" but the high coverage pattern simply gains intensity in the six beams. Alvey and Yates interpret this as the free rotation of PF_3 at low coverage and that free rotation is blocked at high coverage by the interlocking moieties of F. The temperature effect is reversible because if the sample is cooled back to 85 K the beam structure returns at low coverage. At high coverage however a central beam has also appeared whose explanation will follow. Alvey, Yates, and Uram[5] have modeled this hindered rotation with a sixfold barrier to rotation of 10 meV, and they fit the data at both 85 K and 275 K fairly well. Thus we see in a very direct manner the spinning rotation of a surface molecule.

Our focus now, however, is on the electron beam induced effects. For larger fluences of electrons there is a profound change in the pattern. Figure 19 shows the result of 2.9×10^{15} electrons/cm^2 at 55 eV on the high coverage pattern. The resultant pattern is characterized by a large central peak and six wider angle beams. Note that the six beams on

Electron Induced Conversion of PF_3 to PF_x Species on Ni(111): F^+ ESDIAD

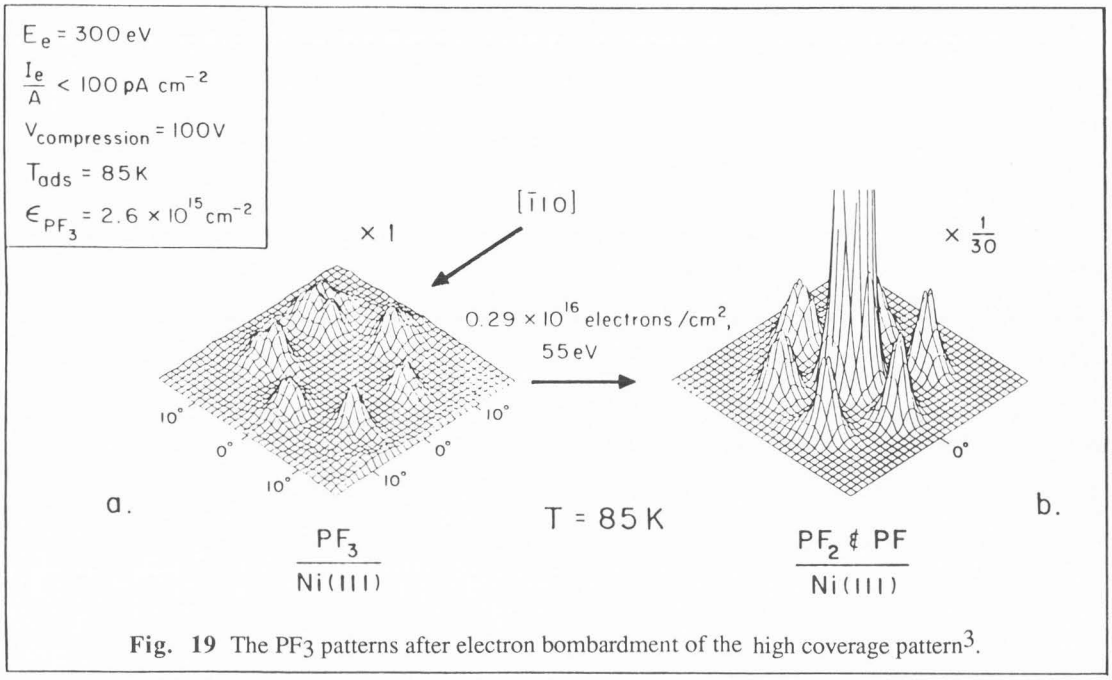

Fig. 19 The PF_3 patterns after electron bombardment of the high coverage pattern[3].

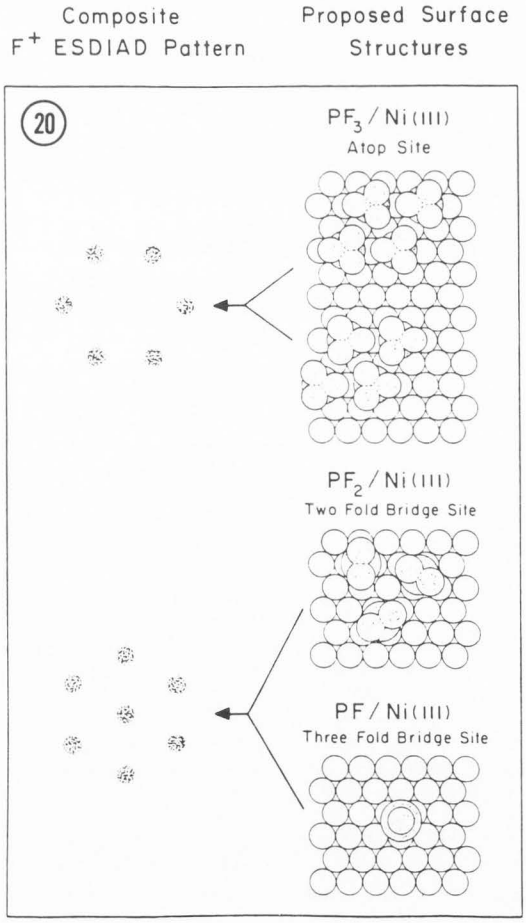

the outer periphery have rotated by 30° from the earlier pattern. Ball models of the surface configurations that could lead to these patterns are shown in Fig. 20. In the model we see how the orientations of different domains of PF_3 in atop sites will lead to the six beam pattern that was seen in Fig. 18. On the other hand PF_2 is more likely to be found on bridging sites since it forms twofold bridging ligands in inorganic reactions. Alvey and Yates[3] proposed the model of locating PF_2 on twofold bridging sites and PF on threefold bridging sites. Thus the PF_2 has three orientations that can lead to the six beam pattern rotated 30° from the original pattern. The PF entities are then in vertical orientations with the F pointing up. It is this last configuration that leads to the strong central peak.

If this surface is now heated to 275 K and then cooled back to 85 K the pattern is irreversibly altered. The six side beams will be much weaker and less localized. Heating to 525 K removes all ESD activity even though one must heat to 650 K to remove the PF_2 species. We conclude that the F^+ yield in these data is from PF or PF_2 on the surface. While F is on the surface the fact that heating to 525 K destroys the ESD yield but further heating does yield PF_2 species, suggests that those F moieties do not yield F^+. The heating to 525 K has probably dissociated the surface species to P and F on the surface. Subsequent heating causes recombination to give the thermal release of PF_2 above 650 K . Thus F on this surface does not yield F^+ ions. These conjectures need to be confirmed by one of the surface spectroscopies such as EELS or Reflection Infra-red Spectroscopy.

Fig. 20 A ball model of the surface configuration that is consistent with the data seen in Fig. 19.

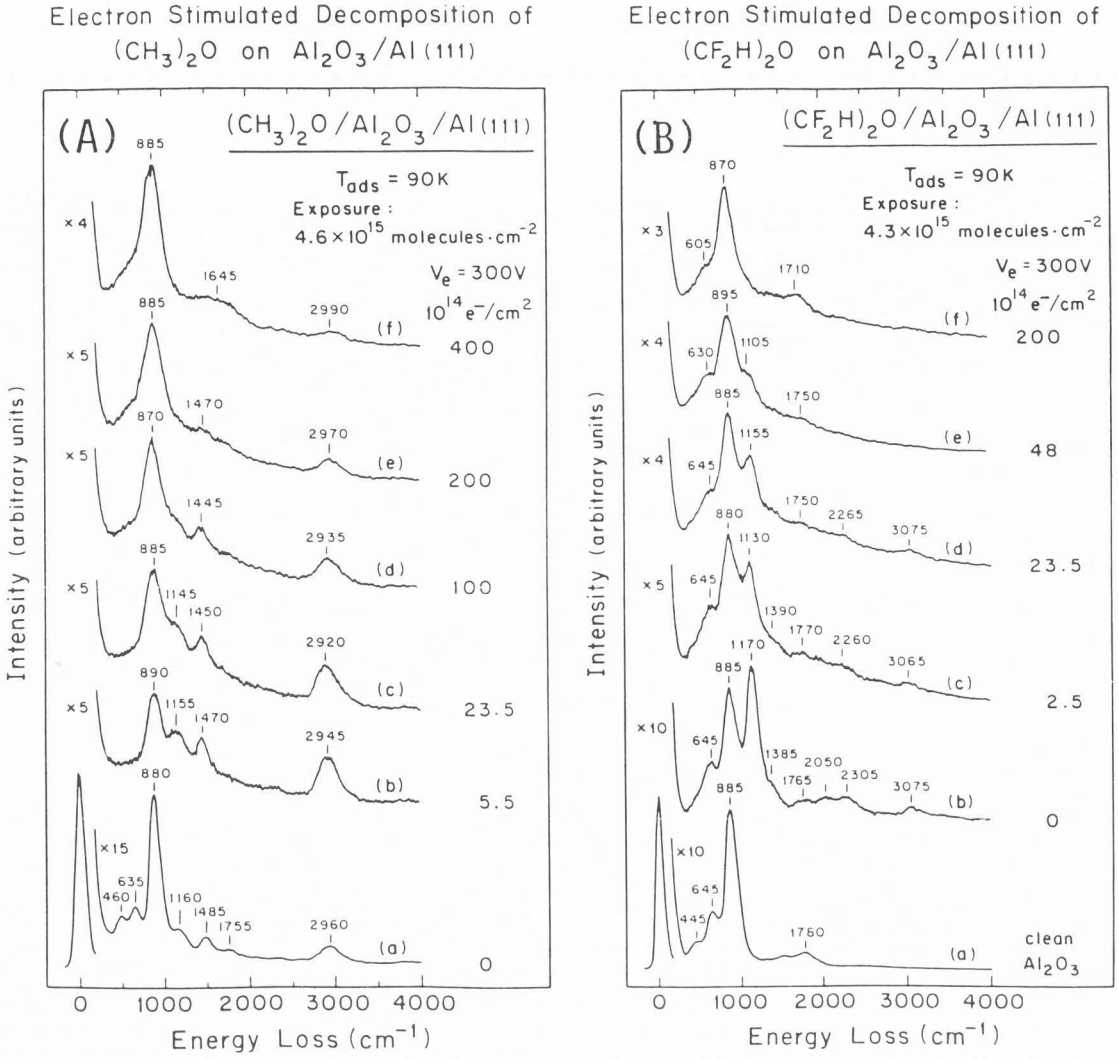

Fig. 21 Vibrational spectra (EELS) recorded following electron bombardment of an adsorbed layer of A.) $(CH_3)_2O$ on Al_2O_3 and B.) $(CF_2H)_2O$ on Al_2O_3[20].

Other studies that have been done on electron beam induced chemical changes include a study of the decomposition of dimethyl ether ($(CH_3)_2O$) and bis(difluoromethyl) ether ($(CF_2H)_2O$) on the alumina surface under electron irradiation[20]. These ethers adsorb to the surface through the oxygen lone pairs. The prolonged irradiation of either molecule leads to a bonding of either carbon or fluorine to the surface. The fluorinated surface is extremely stable. Subsequent heating to 700 K or electron fluences of 1.4×10^{17} e^-/cm^2 at 300 eV did not alter the population of Al-F bonds. Figure 21 shows the progression in the EELS spectrum for this work. The ν(C-F), δ(C-H), and ν(C-H) are seen to lose intensity with electron bombardment. The progressive loss of the ν(C-H) feature, at ~3000cm^{-1}, suggests that this is another example of dissociation that we saw for NH_3 and PF_3, that is, the progressive loss of hydrogen moieties as seen in this case by losses in the EELS spectrum.

Conclusions

We have seen several examples of electron induced behavior. The excitation process at the surface is also a process that leads to other chemical changes. Many electronic states are possible upon excitation. Some of these states lead to desorption mechanisms that deplete the surface of specific species. During the desorption process curve crossing interactions may occur such as reneutralization where the product may escape the surface or it may be recaptured by the surface. All of these reaction possibilities lead to changes in the chemical composition of the surface. The desorbing fragments give us a graphic view of the surface configuration and I have shown examples of surface phase changes as manifest in tilted species as seen by ESDIAD. This method of imaging molecular orientations on surfaces then became a tool to observe surface change as a result of electron beam effects. The common theme of all these studies was the progressive loss of the outer moieties of the species leading to a surface remnant that was fairly stable. I have used examples of metal, semiconductor and insulator surfaces and we have found that although different species are bound to different surfaces those bound species are altered by electron bombardment in a very similar manner. There are, of course, many other electron beam effects that I have not addressed. Higher incident

energies can lead to surface damage which can create new reactive sites for chemical change. The whole realm of sputtering processes is another area that can have strong effects on the surface chemistry. It has been my intent to focus on those microscopic processes that may be fundamental to a wide variety of electron beam interactions on surfaces.

References

1. Alvey MD, Dresser MJ, Yates JT Jr. (1986) Conformational Changes in Chemisorbed CO on Ni(110) Due to Molecular Interactions: An ESDIAD Study, Surf. Sci. **165**, 447-465

2. Alvey MD, Dresser MJ, Yates JT Jr.(1986) Metastable Angular Distributions from Electron-Stimulated Desorption, Phys. Rev. Lett.. **56**, 367-370

3. Alvey MD and Yates JT, Jr. (1988) Structure and Chemistry of Chemisorbed PF_3, PF_2, and PF on Ni(111): An ESDIAD Study, J. Amer. Chem. Soc. **110**, 1782-1786

4. Alvey MD, Klauber C, Yates JT Jr. (1985) Surface Bonding of the NH_3 and NH_2 species to Ni(110), J. Vac. Sci. Technol. **A 3**, 1631-1632 and references therein.

5. Alvey MD, Yates JT Jr, Uram KJ. (1987) The Direct Observation of Hindered Rotation of a Chemisorbed Molecule: PF_3 on Ni (111), J. Chem. Phys. **87**, 7221-7228

6. Avery NR, (1981) Electron Energy Loss Spectroscopic Study of CO on Pt(111), J. Chem. Phys. **74**, 4202-4203

7. Bassignana IC, Wagaman K, Küppers J, Ertl G. (1986) Adsorption and Thermal Decomposition of Ammonia on a Ni(110) Surface - Isolation and Identification of Adsorbed NH_2 and NH, Surf. Sci. **175**, 22-44

8. Bozack MJ, Dresser MJ, Choyke WJ, Taylor PA, Yates JT Jr. (1987) Si-F Bond Direction on Si(100 - A Study By ESDIAD, Surf. Sci. **184**, L332-L338

9. Bozack MJ, Taylor PA, Choyke WJ, Yates JT Jr. (1986) Chemical Activity of the C=C Double Bond on Silicon Surfaces, Surf. Sci. **177**, (1986), L933-L937

10. Danielson LR, Dresser MJ, Donaldson EE, Sandstrom DR. (1978) Effects of an Electron Beam on Adsorption and Desorption of Ammonia on Ruthenium (0001), Surf. Sci. **71**, 615-629

11. Dresser MJ, Alvey MD, Yates JT Jr. (1986) An Enhanced Electron-Stimulated-Desorption Ion Angular Distribution Method For Imaging Molecular Orientations of Adsorbed Species, J. Vac. Sci. Tech. **A4**, 1446-1450

12. Dresser MJ, Alvey MD, Yates JT Jr. (1986) Enhancement of the ESDIAD Method For Imaging Bond Directionality in Chemisorbed Species, Surf. Sci. **169**, 91-103

13. Dresser MJ, Taylor PA, Wallace RM, Choyke WJ, Yates JT Jr. (1989) The Adsorption and Decomposition of NH_3 on SI(100) - Detection of the NH_2 Species, Surf. Sci. **218**, 75-107

14. Feibelman PJ, Knotek ML. (1978) Reinterpretation of Electron Stimulated Desorption Data from Chemisorption Systems, Phys. Rev. B **18**, 6531-6539

15. Johnson AL, Walczak MM, Madey TE. (1988) ESDIAD of First-Row Protic Hydrides Adsorbed on Si(100): Structure and Reactivity, Langmuir **4**, 277-282

16. Kiskinova M, Szabo A, Lanzillotto A-M, Yates JT Jr. (1988) Electron Stimulated Desorption From CO Chemisorbed on Pt(111): A Dynamical Study of Positive Ion and Metastable CO Emission, Surf. Sci. **202**, L559-L567

17. Kiskinova M, Szabo A, Yates JT Jr. (1988) Compressed CO Overlayers on Pt(111) - Evidence for Tilted CO Species at High Coverages by Digital ESDIAD, Surf. Sci. **205**, 215-229

18. Menzel D, Gomer R. (1964) Desorption From Metal Surfaces by Low Energy Electrons, J. Chem. Phys. **41**, 3311-3328

19. Miskovic Z, Vukanic J, and Madey TE. (1986) Calculations of Reneutralization Effects in ESDIAD, Surf. Sci. **169**, 405-413

20. Ng L, Chen JG, Basu P, Yates JT Jr. (1987) Electron-Stimulated Decomposition of Alkyl and Fluoroalkyl Ethers Adsorbed on Al_2O_3, Langmuir **3**, 1161-1167

21. Ramaker DE, White CT, Murday JS. (1982) On Auger Induced Decomposition/Desorption of Covalent and Ionic Systems, Phys . Lett. **89A**, 211-214

22. Redhead P. (1964) Interaction of Slow Electrons with Chemisorbed Oxygen, Can. J. Phys. **42**, 886-905

Discussion with Reviewers

D. E. Ramaker: The author suggests that the CO^* and CO^+ desorption from CO/Ni(110) result from a common 2h1e excitation, the CO^* then resulting from neutralization of CO^+. If this is true, then the angular distribution of these two species should directly reflect the effects of image charge and neutralization (i.e., I would expect the image charge effect to make the fwhm of the CO^+ larger and the neutralization to make it smaller than that for CO^*). How do the fwhm compare for these two species, and does this comparison lead to the same conclusions as those reached by Miskovic et al[19]?

Author: The angular distributions are reported in reference [2]. The angular distribution of CO^* is not azimuthally isotropic from the Ni(110) surface. The fwhm along the $[1\bar{1}0]$ surface direction is 22° and along the [001] direction it is 14°. For the ionic patterns there is a much smaller anisotropy, we found that the fwhm was ~ 16° in the $[1\bar{1}0]$ direction and ~15° in the [001] direction. The interpretation of the ellipticity in the CO^* pattern is that the reneutralization probability is larger along the $[1\bar{1}0]$ rows than it is in the orthogonal [001] direction, thus yielding the enhancement in neutral emission in that direction. The calculation of Miskovic et al[19] did not specifically address the issues of fwhm for normal emission but rather predicting the peak position of the distribution for off axis emission. I think we can infer, however, from that work that at angles near normal emission, as we have here, the two effects, (image charge attraction and reneutralization), are generally self cancelling so that the difference in the distributions may be only minor. The difference reported by Alvey et al[2] is seen as evidence that the surface asymmetry of the Ni(110) surface is strong enough to amplify one component of these cancellations and to bring into question the assumption of Miskovic et al[19] that the reneutralization probability is isotropic. Clinton and Pal, (Clinton WL, Pal S. (1987) Influence of Surface Corrugations on Electron-stimulated Desorption: Angular Distributions of Ions and Neutral Atoms from Ni(110)-CO, Phys. Rev. B **35**, 2991-2994), have actually calculated the effect of surface corrugation on the reneutralization probability and found that the enhanced metastable emission along the $[1\bar{1}0]$ direction is consistent with that model.

D. E. Ramaker: I would expect the Coulomb force existing in a 2h state to be directly along the original bond direction. However, this does not necessarily follow for desorption from a 2h1e state, since the 2h1e equilibrium geometry may not be the same as it was in the ground state. Does any evidence exist for any system that desorption does not occur along the original bond direction?

Author: I am not aware of any such evidence. However, since much of the interpretation of workers in this area

assumes this fact, it is possible that an exception may have been missed. In 1982 Ted Madey et al (Madey TE, Netzer FP, Houston JE, Hanson DM, Stockbauer R, (1983) The Determination of Molecular Structure at Surfaces Using Angle Resolved Electron- and Photon-Stimulated Desorption, in: Desorption Induced by Electronic Transitions, DIET I, Tolk NH, Traum MM, Madey TE, Tully JC, (ed) Springer Series in Chemical Physics **24** Springer-Verlag, Heidelberg, 120-138) presented a thorough comparison of bond angles determined by ESDIAD as compared to other orientation sensitive techniques. At that point there were no exceptions and many examples of good agreement. A more recent and precise comparison has been made for this specific system by Wesner et al, (Wesner DA, Coenen FP, Bonzel HP. (1988) Tilted CO on Clean and Potassium-covered Ni(110): Adsorbate Orientation from Polar-angle X-ray-photoelectron Diffraction, Phys. Rev. Lett. **60**: 1045-1048). In this work the authors determine the angle of tilt of CO on Ni(110) at high coverage by the use of x-ray photoelectron diffraction and find that it is 21° which is in very close agreement with the 19° of Alvey et al's[1] ESDIAD measurement. It is certainly experimentally evident that if our assignment of the 2h1e state is correct that the desorption trajectories are as precisely focused relative to the surface normal as are those of other excitations such as the excitations that yield the O^+ ions.